13 September 1996

ELSEVIER

Chemical Physics Letters 259 (1996) 568–573

CHEMICAL PHYSICS LETTERS

Metal particle catalysed production of nanoscale BN structures

M. Terrones [a], W.K. Hsu [a], H. Terrones [b], J.P. Zhang [c], S. Ramos [b], J.P. Hare [a], R. Castillo [b], K. Prassides [a], A.K. Cheetham [c], H.W. Kroto [a], D.R.M. Walton [a]

[a] *School of Chemistry and Molecular Sciences, University of Sussex, Brighton BN1 9QJ, UK*
[b] *Instituto de Física, UNAM, Apartado Postal 20-364, México, D.F. 01000, México*
[c] *Materials Research Laboratory, University of California, Santa Barbara, CA 93106, USA*

Received 17 June 1996

Abstract

Graphite-like nanostructures including nanotubes and encapsulated polyhedral particles have been obtained by arcing hexagonal boron nitride (h-BN) and tantalum in a nitrogen atmosphere. High resolution electron microscopy (HRTEM), electron energy loss spectroscopy (EELS) and X-ray diffraction studies have been used to study these new materials, which contain B:N ratios of $\approx$ 1:1. The observations reveal interesting new information on the dynamics of metal cluster catalysed nanostructure formation. The structures provide strong circumstantial evidence for the presence of B_2N_2 squares at the tips, in addition to B_3N_3 hexagons in the main body of the tubes.

1. Introduction

Following the discovery [1] and bulk production [2] of fullerenes, novel graphitic structures (e.g. carbon nanotubes [3,4], graphitic onions or giant concentric fullerenes [5,6]) were observed by HRTEM in the deposits generated at the cathode during the arc-discharge between graphite electrodes in inert atmospheres [2–4,6]. Lately, new methods for producing fullerenes and graphitic nanostructures have been developed involving pyrolysis [7–10] and combustion [11] of hydrocarbons, laser irradiation of graphite [12] and electrolysis using graphite electrodes in molten salts [13]. Moreover, it has proved possible to encapsulate metal oxides [14], ferromagnetic materials [15] and superconducting nanocarbides [16–18] in nanotubes and graphitic nanoparticles. These new materials may have potential applications in magnetic data storage devices, toners and inks for xerography [15], superconducting nano-circuits in electronics, etc. Additionally, pyrolytic methods have also been used to generate helical nanotubes [19,20], hemitoroidal nanotube caps [10,21,22] and bent nanotubes [22,23]. Here the introduction of heptagons, in addition to pentagons, into the predominantly hexagonal network appears to be responsible for the negative curvature [20,24,25].

Other layered materials, such as MoS_2 [26], WS_2 [27], BC_2N [28,29], BC_3 [28], BCN [30] and BN [31], have recently been shown to form closed concentric-shell nanoparticles and nanotubes. The production of these novel graphite-like nanostructures, which may possess interesting mechanical and electronic properties, opens up a new era in materials science and nanoscale engineering.

In this Letter we describe the creation of nanoscale materials from boron nitride by arc discharge techniques. Nanostructures have been observed which

PII S0009-2614(96)00773-7

are not only novel, but also provide information on which to base a theoretical understanding of the dynamics of the catalytic growth process.

2. Experimental

Samples were prepared using the arc-discharge dc generator employed for fullerene production. The anode consisted of a tantalum (99.9%) tube (4 mm id, 5 mm od; Goodfellow Co.) press-filled with boron nitride powder (99%, Aldrich Co). The cathode consisted of a water-cooled Cu disk (200 mm diameter).

Before arcing, the chamber was purged twice with nitrogen (air products 99.9% purity) and then filled with nitrogen at ≈ 200 Torr. During arcing the electrical conditions varied between 25–40 V and 80–150 A. The gap between the electrodes was maintained at ≈ 1 mm. As the anode rod was consumed, a grey deposit formed on the cathode (reaction time ≈ 2 min). A few mg of this deposit were sonicated in acetone for 5 min and then placed on a perforated carbon grid and the solvent was allowed to evaporate. TEM and HRTEM measurements were made using: JEM4000 (400 kV), Hitachi 7100 (125 kV) and a JEOL 2010 microscope equipped with a high resolution pole piece (0.19 nm at 200 kV). A Gatan imaging filter (GIF) system with a 1024×1024 CCD camera [32] is attached to the latter microscope for image recording and EELS spectrum collection. This microscope was operated at 200 kV with a LaB6 cathode, and the beam size for EELS study was less than 3 nm. We used 0.3 eV dispersion for EELS fine structure study while 0.5 eV dispersion was chosen to obtain the spectrum in a larger energy range (about 500 eV) with a collecting angle of about 5 mrad for elemental ratio calculation. Since the thickness of the tubes is much smaller than the mean free path of this material (the kinematical consideration), an ideal single scattering distribution is applied to EELS spectrum calculations.

3. Results and discussion

HRTEM and TEM studies show that the grey deposits on the cathode contain long (4–6 μm), very thin (1.3–4.5 nm od) nanotubes ($\approx$ 2–8 layers) as well as polyhedral encapsulated particles (Fig. 1). X-ray powder diffraction analysis (Siemens D-5000, Cu-K_α radiation) of the deposits clearly show the presence of hexagonal boron nitride (interlayer spacing ≈ 3.33 Å) and hexagonal Ta_2N in the bulk of the material. The exact nature of the catalytic particle is currently the subject of investigation. Preliminary electron diffraction (ED) data suggest the presence of a phase isostructural with hexagonal TaB_2; however, only a very small amount of this phase is evident in the XRD profiles. It is possible that amorphous BN starts to agglomerate at the metal or metal boride/nitride particle, producing tubules and polyhedral particles. We have also observed nanotubes with square and open-triangular caps, with no metal particles. In the following section a possible mechanism for the formation of these structures is presented.

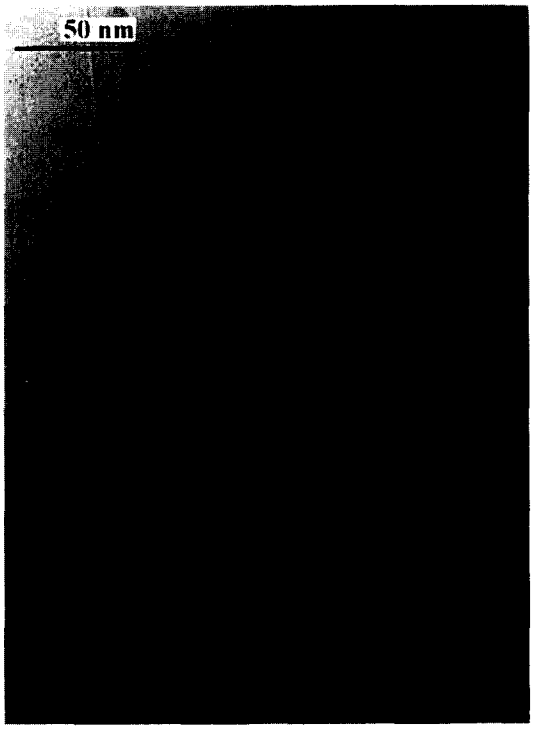

Fig. 1. Moderate resolution TEM image showing a fairly representative sample of nanotubes and polyhedral particles containing encapsulated material. The tubule with a metal particle on the tip in the clear is shown in more detail in Fig. 3a.

Fig. 2 shows a representative EELS spectrum of a nanotube. Ionisation edges are observed at ≈ 188 eV

and 399 eV which correspond to the characteristic K-shell ionisation edges of boron and nitrogen. For the boron and nitrogen, the sharply defined fine structural features of the π^* and σ^* pre-ionisation edges are characteristic of sp^2 hybridisation seen in graphite-like structures. The EELS measurements indicate that the nanotubes exhibit the expected boron:nitrogen ratio of $\approx$ 1:1 (BN).

3.1. BN structure growth catalysed by metal particles

A typical medium resolution TEM image is shown in Fig. 1. Many of the BN tubes are quite long (≈ 5 μm), relatively straight, and invariably ($\leqslant 85\%$) have a metal particle attached to one end (Fig. 1). We have discovered at least three types of configuration involving catalytic particles and resulting nanostructures/nanotubes. In some cases the catalytic particle (which appears to be TaB_2 by ED) is completely encapsulated within the tip of a nanotube, similar to observations reported elsewhere [17,18]. However, in Fig. 3a and 3b two different configurations are observed. These reveal key features relating to the nanotube creation process. In Fig. 3a. we see the end of a near perfect triple-walled nanotube (seen also under low resolution in Fig. 1) and its catalytic particle. The structure observed is quite fascinating as the tube appears to have extruded from one side

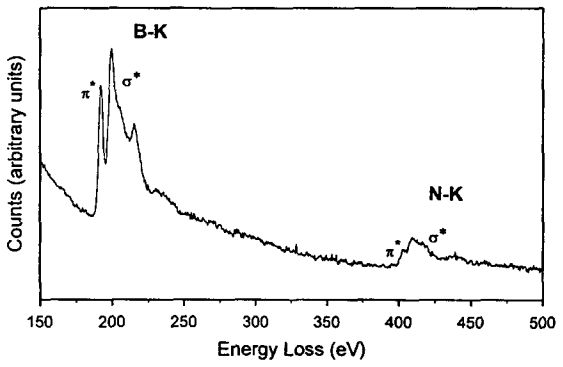

Fig. 2. EELS spectra showing ionisation edges at $\approx 188 \pm 2$ eV and 399 ± 2 eV which correspond to the characteristic K-shell ionisation edges of boron and nitrogen respectively. The structure of these sharp features indicates that the B and N bonding involves sp^2 hybridisation as in graphite and normal hexagonal BN.

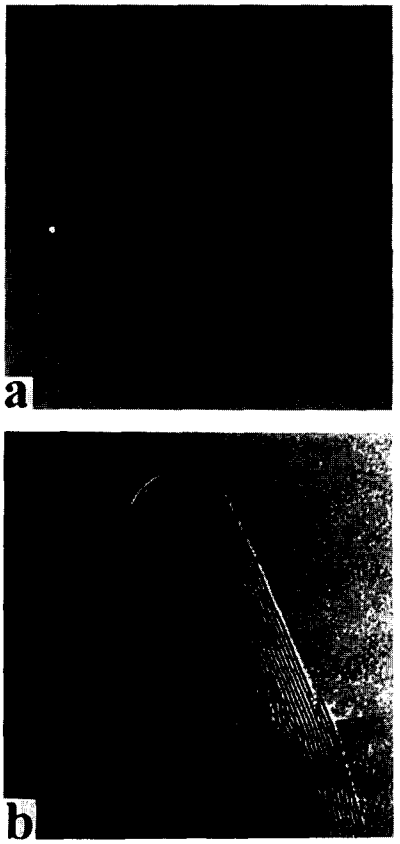

Fig. 3. (a) HRTEM image from a triple walled nanotube exhibiting a metal particle at the tip (see also Fig. 1). (b) Metal particle with BN 'graphitic' layers attached. It is important to note that the metal particle may be responsible for the nanotube growth by subsequent agglomeration of amorphous BN around it.

of the catalytic particle. One interpretation of the distorted sections (adjacent to the particle) is that they are flattened tube sections which appear to gain perfection at some distance from the particle. Thus, they appear to become more cylindrical as they are released from the particle's surface. A further important observation is that on the opposite side to the nanotube formation zone there appears to be a bulky deposit which is probably amorphous BN.

A possible mechanistic scenario is that amorphous BN material aggregates on one side of the metal particle and enters into a form of crystalline Ta–B–N solid solution. The B and N atoms then effectively migrate through the metal; localised thermodynamic

conditions in the nanotube construction zone then favour segregation of layered crystalline BN. The atoms are sufficiently well organized by interaction with the Ta that hexagonal layers are able to self-assemble on the opposite side of the particle.

In Fig. 3a approximately six layers appear to have formed. One possible explanation of the apparent convergence of the layers, as they approach the particle, is that edge-sealing (or an effective equivalent) has occurred between the edges of layers 1 and 6, 2 and 5, as well as 3 and 4. This may occur at the same time as the layers form in the organization zone on the side of the particle. As further BN material segregates it lays down epitaxially at the rim of the flattened tube and, as more material forms, the middle layers are able to separate. As further tubular BN material is shed from the particle, the original structure, consisting of three flattened concentric cylinders, is created and upon spooling away from the formation zone, it springs out – reminiscent of a piece of flattened rubber tubing that has been released from compression. The result is a perfectly cylindrical nanotube created by a remarkable exercise in nanoscale self-assembly. It is difficult to envisage a simpler process at the stage.

Fig. 4. (a) HRTEM image of two overlapping nanotube caps, in which one of them shows a clear square cap. This may be explained by the introduction of four membered rings in the hexagonal BN network. (b) HRTEM image of a cone-shaped partly open cap.

This, or a somewhat similar, mechanistic scenario gains a measure of support from a second structure, shown in Fig. 3b. Here a laminated BN sheet – rather than a tube – appears to have been created on the side of a catalytic particle. The structure appears to be a laminated strip with perhaps a curved arc cross-section. Such a curved cross-section would explain the excellently well-resolved and continuous TEM lines in Figure. 3b, which correspond to the laminations. There is no obvious evidence that the structure is a closed tubule. The occasional disappearance of outer-edge lines is consistent with a set of curved sheets which lie at a slight angle to the electron beam and is inconsistent with a tubular construction which, if more-or-less perfect, would not exhibit disappearing lines. This particular project has thus shed, and is continuing to shed, fascinating new light on the dynamic factors which govern the nanotube creation process.

3.2. BN nanotube caps

Another interesting feature is the presence of nanotubes without metal particles at their tips. Some of these tubes exhibit closed-flat caps, whereas, others possess open-triangular caps (Fig. 4a and 4b). These structural phenomena are rather different from those encountered in carbon nanotubes. In conformity with Euler's equation for even-membered rings ($12 = 2n_4 - 0n_6 - 2n_8$) a closed, flat structure can arise at one end of a BN nanotube if, instead of pentagons, either three squares (Fig. 5a, 5b) or four squares and one octagon (Fig. 5c, 5d) are introduced in a symmetrical array into the BN hexagonal network.

It is interesting to note that square, or approximately square cross-sections are statistically quite

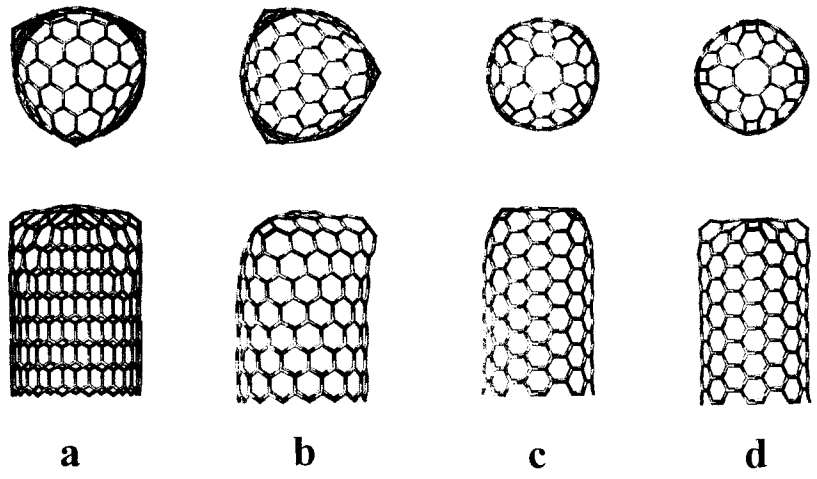

Fig. 5. (a and b) Molecular model of a BN tubule cap in which three squares are equilaterally distributed over a zig-zag type hexagonal tubule. Rotations along the tube axis show that the square shape varies and is not always a sharp well defined square. (c and d) Another BN nanotube cap containing four squares and one octagon (armchair conformation). Rotation of this tube shows that a sharp square shape is always preserved under any rotation along the fibre axis.

common in our study, and very unusual in carbon nanotubes. One possible reason is that as the tube grows, the occasional occurrence of a *single* four-membered ring leads to the propagation of subsequent layers more-or-less at right-angles to the cylindrical walls. Then relatively rapid closure by a facile annealing process may occur as the surface meets the opposite side of the tube. The key point here is that the occurrence of a single four-membered ring will tend to lead to closure by a *sharp* relatively square cross-section cap. For carbon nanotubes, where pentagons are the preferred non-hexagonal ring, the advent of a *single* pentagonal disclination leads to a cone.

The open-triangular cap (Fig. 4b) may form due to the frustration in creating four-membered BN rings along the tubule tip thus resulting in open structures. It is important to note that the encapsulated polyhedral particles in our experiments also exhibit sharp continuous corners where non-hexagonal or odd-membered rings appear to be present.

4. Conclusions

In addition to the closed carbon structures, it appears that BN ($\approx$ 1:1 ratio) can also form fullerene-like materials, including nanotubes and polyhedral particles, in which metal-catalysed processes appear to be involved. We have observed that the number of layers in the BN nanotubes is much less when compared with carbon nanotubes produced by plasma arcs or pyrolytic methods. This might be due to shorter reaction times for the Ta/BN experiment ($\approx$ 2 min). The present Letter provides evidence for the catalytic formation of BN nanotubes, in which the metal particles are responsible for the BN accretion and subsequent growth of relatively perfect cylindrical tubules by a nanoscale self-assembly process. In addition to this catalytic process, we have found BN nanotubes which do not contain any catalytic metal particle either on or inside the tips. These tubules show unusual caps (closed square and open triangular) which are thought to possess four- and perhaps also eight-membered rings in the predominantly hexagonal BN network. It is possible that other layered materials may also form closed, bent and curled nanotubes and/or closed shell nanoparticles. The occurrence of square cross-section caps is a characteristic of BN nanotubes which differ from those of carbon tubes. This can be rationalised on the basis of a preference for 4 membered rings which may be due to the expected chemical bonding requirement that B and N atoms alternate so leading to the absence of odd membered rings in the network.

Acknowledgements

We are grateful to Luis Rendón (UNAM-México) for providing the HRTEM facilities. We thank CONACYT-México for funding grants 3348-E and 088P-E (to HT) and a scholarship (MT), the ORS scheme for scholarships (MT and WKH), the Royal Society and the ESRC for financial support. We are particularly grateful to Dr. Alfred Bader and Dr. Peter Doyle (ZENECA) for generous assistance.

References

[1] H.W. Kroto, J.R. Heath, S.C. O'Brien, R.F. Curl and R.E. Smalley, Nature 318 (1985) 162.
[2] W. Krätschmer, L.D. Lamb, K. Fostiropoulos and D.R. Huffman, Nature 347 (1990) 354.
[3] S. Iijima, Nature 354 (1991) 56.
[4] T.W. Ebbesen and P.M. Ajayan, Nature 358 (1992) 220.
[5] S. Iijima, J. Cryst. Growth 5 (1980). 675.
[6] D. Ugarte, Nature 359 (1992) 707.
[7] R. Taylor, G.J. Langley, H.W. Kroto and D.R.M. Walton, Nature 366 (1993) 728.
[8] C. Crowley, H.W. Kroto, R. Taylor, D.R.M. Walton, M.S. Bratcher, P.C. Cheng and L.T. Scott, Tetrahedron Lett. 36 (1995) 9215.
[9] M. Endo, K. Takeuchi, M. Shiraishi and H.W. Kroto, J. Phys. Chem. Solids 54 (1993) 1841.
[10] M. Endo, K. Takeuchi, K. Takahashi, H.W. Kroto and A. Sarkar, Carbon 33 (1995) 873.
[11] J.B. Howard, A.L. Lafleur, Y. Makarovsky, S. Mitra, C.J. Pope and T.K. Yadav, Carbon 30 (1992). 1183.
[12] T. Guo, P. Nikolaev, A.G. Rinzler, D. Tomélnek, D.T. Colbert and R.E. Smalley, J. Phys. Chem. 99 (1995) 10694.
[13] W.K. Hsu, J.P. Hare, M. Terrones, P.J.F. Harris, H.W. Kroto and D.R.M. Walton, Nature 377 (1995) 687.
[14] S.C. Tsang, Y.K. Chen, P.J.F. Harris and M.L.H. Green, Nature 372 (1994) 159.
[15] M.E. McHenry, Y. Nakamura, S. Kirkpatrick, F. Johnson, S. Curtin, M. DeGraef, N.T. Uhfer, S.A. Majetich and E.M. Brunsman, in: *Recent advances in the chemistry and physics of fullerenes and related materials*, Vol. 2, ed. K M. Kadish and R.S. Ruoff (1995) p. 1463.
[16] Y. Murakami, T. Shibata, K. Okuyama, T. Arai, H. Suematsu and Y. Yoshida, J. Phys. Chem. Solids 54 (1994) 1861.
[17] M. Terrones, J.P. Hare, W.K. Hsu, H.W. Kroto, A. Lappas, W.K. Maser, A.J. Pierik, K. Prassides, R. Taylor and D.R.M. Walton, in: Recent advances in the chemistry and physics of fullerenes and related materials, Vol. 2, ed. K M. Kadish and R.S. Ruoff (1995) p. 599.
[18] J.P. Hare, W.K. Hsu, H.W. Kroto, A. Lappas, K. Prassides, M. Terrones and D.R.M. Walton, Chem. Mater. 8 (1996) 6.
[19] S. Amelinckx, X.B. Zhang, D. Bernaerts, X.F. Zhang, V. Ivanov and J.B. Nagy, Science 265 (1994) 635.
[20] H. Terrones, M. Terrones and W.K. Hsu, Chem. Soc. Rev. 24 (1995) 341.
[21] A. Sarkar, H.W. Kroto and M. Endo, Carbon 33 (1995) 51.
[22] M. Terrones, W.K. Hsu, J.P. Hare, D.R.M. Walton, H.W. Kroto and H. Terrones, Phil. Trans. R. Soc. *A* (1995) in press.
[23] D. Bernaerts, X.B. Zhang, X.F. Zhang, S. Amelinckx, G. Van Tendeloo, J. Van Landuyt, V. Ivanov and J.B. Nagy, Phil. Mag. *A* 71 (1995) 605.
[24] A.L. Mackay and H. Terrones, Nature 352 (1991) 762.
[25] H. Terrones, J. Fayos and J.L. Aragón, Acta Metall. Mater. 42 (1994) 2687.
[26] L. Margulis, G. Saltra, R. Tenne and M. Tallanker, Nature 365 (1993) 113.
[27] R. Tenne, L. Margulis, M. Genut and G. Hodes, Nature 360 (1992). 444.
[28] Z. Wen-Sieh, K. Cherrey, N.G. Chopra, X. Blase, Y. Miyamoto, A. Rubio, M.L. Cohen, S.G. Louie, A. Zettl and R. Gronsky, Phys. Rev. B 51 (1995) 11299.
[29] M. Terrones, A.M. Benito, C. Manteca-Diego, W.K. Hsu, O.I. Osman, J.P. Hare, D.G. Reid, H. Terrones, A.K. Cheetham, K. Prassides, H.W. Kroto and D.R.M. Walton, Chem. Phys. Lett. (1996) in press.
[30] O. Stephan, P.M. Ajayan, C. Colliex, P. Redlich, J.M. Lambert, P. Bernier and P. Lefin, Science 266 (1994) 1683.
[31] N.G. Chopra, R.J. Luyken, K. Cherrey, V.H. Crespi, M.L. Cohen, S.G. Louie and A. Zettl, Science 269 (1995) 966.
[32] O.L. Krivanek, A.J. Gubben, N. Dellby and C.E. Meyer, Microsc. Microanal. Microstruct., 3 (1992) 187.